2024

DEVELOPMENT OF GLUTATHIONE-RESPONSIVE DISULFIDE-CONTAINING POLY(BETA-AMINO ESTERS) WITH VARIED HYDROPHILICITY AND ACRYLATE FUNCTIONALITY

Anastasiia Aronova
University of Kentucky, aar230@uky.edu
Digital Object Identifier: https://doi.org/10.13023/etd.2024.353

STUDENT AGREEMENT:

I represent that my thesis or dissertation and abstract are my original work. Proper attribution has been given to all outside sources. I understand that I am solely responsible for obtaining any needed copyright permissions. I have obtained needed written permission statement(s) from the owner(s) of each third-party copyrighted matter to be included in my work, allowing electronic distribution (if such use is not permitted by the fair use doctrine) which will be submitted to UKnowledge as Additional File.

I hereby grant to The University of Kentucky and its agents the irrevocable, non-exclusive, and royalty-free license to archive and make accessible my work in whole or in part in all forms of media, now or hereafter known. I agree that the document mentioned above may be made available immediately for worldwide access unless an embargo applies.

I retain all other ownership rights to the copyright of my work. I also retain the right to use in future works (such as articles or books) all or part of my work. I understand that I am free to register the copyright to my work.

REVIEW, APPROVAL AND ACCEPTANCE

The document mentioned above has been reviewed and accepted by the student's advisor, on behalf of the advisory committee, and by the Director of Graduate Studies (DGS), on behalf of the program; we verify that this is the final, approved version of the student's thesis including all changes required by the advisory committee. The undersigned agree to abide by the statements above.

Anastasiia Aronova, Student

Dr. Thomas Dziubla, Major Professor

Dr. Zach Hilt, Director of Graduate Studies

DEVELOPMENT OF GLUTATHIONE-RESPONSIVE DISULFIDE-CONTAINING POLY(BETA-AMINO ESTERS) WITH VARIED HYDROPHILICITY AND ACRYLATE FUNCTIONALITY

THESIS

A thesis submitted in partial fulfillment of the
requirements for the degree of Master of Science in the
College of Engineering
at the University of Kentucky

By

Anastasiia Aronova

Lexington, Kentucky

Director: Dr. Thomas Dziubla, Professor of Chemical Engineering

Lexington, Kentucky

2024

ABSTRACT OF THESIS

DEVELOPMENT OF GLUTATHIONE-RESPONSIVE DISULFIDE-CONTAINING POLY(BETA-AMINO ESTERS) WITH VARIED HYDROPHILICITY AND ACRYLATE FUNCTIONALITY

Smart biomaterials are becoming promising for therapeutic deliveries due to their ability to respond to changes in the environment. Redox-responsive hydrogels are a promising type of smart polymer that can swell and degrade according to cellular oxidative stress levels. Glutathione, abundant in cells, is crucial in redox-responsive biomaterials, serving as a key reactive molecule. This study explored the degradation kinetics of glutathione-responsive poly(β-amino ester) (PBAE) polymers created through a single-step Michael addition. We examined how disulfide content influences the degradation kinetics of these PBAE networks. Additionally, we investigated how the hydrophilicity and functionality of acrylate affect the degradation of disulfide-containing PBAE systems. These redox-sensitive materials were tested under nearly physiological conditions of reduced glutathione to determine its effects on the swelling and degradation behavior of disulfide-containing PBAE polymers. Based on these findings, we developed disulfide-containing PBAE nanogels.

KEYWORDS: Hydrogel, poly (β-amino ester) (PBAE), disulfide, glutathione, redox, nanogel.

Anastasiia Aronova

(Name of Student)

05/14/2024

Date

DEVELOPMENT OF GLUTATHIONE-RESPONSIVE DISULFIDE-CONTAINING POLY(BETA-AMINO ESTERS) WITH VARIED HYDROPHILICITY AND ACRYLATE FUNCTIONALITY

By
Anastasiia Aronova

Dr. Thomas Dziubla
Director of Thesis

Dr. J. Zach Hilt
Director of Graduate Studies

05/14/2024
Date

ACKNOWLEDGMENTS

I sincerely thank my advisor and committee chair, Dr. Thomas Dziubla, for his continuous support, patience, guidance, motivation, and immense knowledge. I also want to thank my committee members, Dr. J. Zach Hilt, Dr. Steve Rankin, and Dr. Jason DeRouchey, for their useful comments, remarks, and engagement throughout my studies. I would also like to thank Dr. Gosia Chwatko for her valuable advice and encouragement. Additionally, I wish to acknowledge my lab mates who helped me along the way: Jamie A. Ammar, Alea Smith, and Dr. Kelley Weigman.

Finally, I thank my friends and family who supported me on this journey. I am very grateful to my husband, Sulaiman Dhameri, for his patience, continuous encouragement, and valuable insight.

TABLE OF CONTENTS

LIST OF FIGURES

List of abbreviations

ACN	acetonitrile
DEGDA	diethylene glycol diacrylate
DMSO	dimethyl sulfoxide
CMA	curcumin multiacrylate
CystA	cystamine
GSH glutathione	glutathione
ROS reactive oxidative species	reactive oxidative species
2-ME 2-mercaptoethanol	2-mercaptoethanol
PEG400DA	polyethylene glycol diacrylate (Molecular weight 400)
TTD	4,7,10-trioxa-1,13-tridecanediamine
TMPTA	Trimethylolpropane

CHAPTER 1. EXECUTIVE SUMMARY

The overall goal of this project is to investigate the impact of acrylate functionality and hydrophilicity on the properties of the resulting disulfide-containing poly (beta-amino esters) (PBAE) networks, evaluate their responsiveness to glutathione, and utilize these findings to develop disulfide-containing PBAE nanogels. Here, we evaluate the impact of acrylate hydrophilicity by comparing swelling and degradation rates in physiological levels of glutathione of disulfide-containing PBAE networks made with diethylene glycol diacrylate and polyethylene glycol diacrylate. Additionally, we assess the impact of increased acrylate functionality by incorporating a branched diacrylate into the PBAE network. Lastly, we utilize these approaches' key findings and limitations to develop novel disulfide-containing nanogels.

CHAPTER 2. BACKGROUND

2.1 Redox-responsive biomaterials

In recent years, there has been a significant advancement in the design and development of biomaterials, featuring complex structures and dynamic functions that interact effectively with biological systems, enabling them to perform specific, advanced functions within the body [1-5] Stimuli-responsive biomaterials are a class of biomaterials that can respond to changes in their environments, which can include pH, temperature, light, and others. These smart materials are advantageous due to their ability to provide more controlled response and therapeutic release.

There is a growing interest in tailoring biomaterials that can respond to or mitigate the impact of oxidative stress on the cell. Oxidative stress is a complex mechanism that produces an imbalance of free radical generation and the body's ability to counteract and neutralize them. While some reactive oxygen species (ROS) are a natural byproduct of cellular metabolism and do not pose a threat, an excess free radical generation caused by environmental factors such as UV light, radiation, pollution, and chronic inflammation often results in overwhelming antioxidant capacity, leading to an imbalance. This ROS imbalance can cause cellular and tissue damage and is a contributory factor to multiple diseases, such as neurodegenerative diseases, cardiovascular diseases, diabetes, and various cancers. Glutathione (GSH) is particularly important when it comes to cellular free radical defense. At concentrations of 1-10mM, it is one of the most abundant chemicals found in the cytosol of mammalian cells[6, 7]. It regulates cellular redox homeostasis and protects cells from lipid peroxides, reactive oxygen and nitrogen species, and various xenobiotics, (Figure 2.1) [8-11].

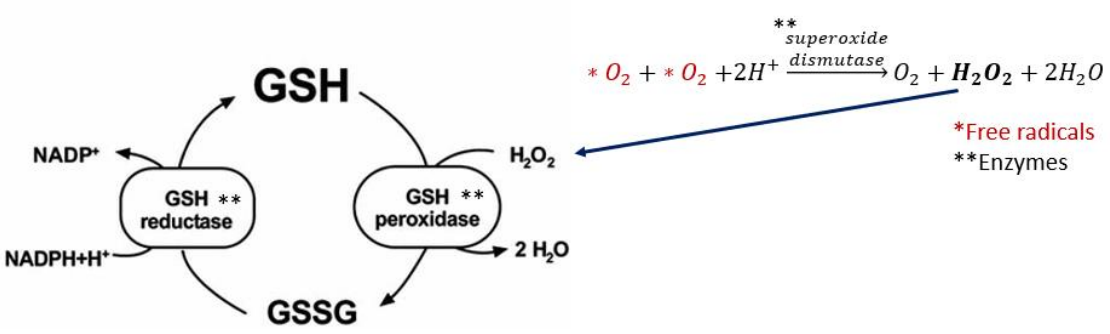

Figure 2.1 Free radical neutralization and recycling mechanism of GSH.

Moreover, the extracellular concentration of GSH is very low (2-20 μM, in plasma), and the thiol group enables GSH to serve as a cellular target for redox-sensitive moieties [12, 13]. Consequently, there has been a growing interest in developing GSH-responsive polymers for targeted delivery to the cytosol, particularly using disulfide-containing biomaterials[14-16].

2.2 Tunable PBAE systems

The versatility, responsiveness, and biodegradability of PBAE polymers have garnered significant attention due to their low cytotoxicity and the presence of β-amino ester linkages, which allows for hydrolytic degradation. The ease of synthesis and tunable degradation also make PBAE polymers an excellent material for biomedical applications such as drug delivery, gene therapy, and tissue repair [17-19]. This process has led to the development of extensive libraries of PBAE-based materials, each with unique properties, by using varied acrylate and amine monomers. For instance, Muralidharan et al. explored the effects of alkene and amine chemistries on forming PBAE diacrylate macromers. Their research found that the alkene backbone's molecular weight and hydrophilicity significantly influenced the mechanical properties, degradation mode, and swelling

capacity. The gels made with low molecular weight, 1,4-butanediol diacrylate, had substantially lower swelling ratios and significantly longer degradation times than those made with polyethylene glycol diacrylate [20]. In our previous work, we pioneered the development and investigation of PBAE systems made with low-molecular-weight diethylene glycol diacrylates and linear diamines (Figure 2.2).

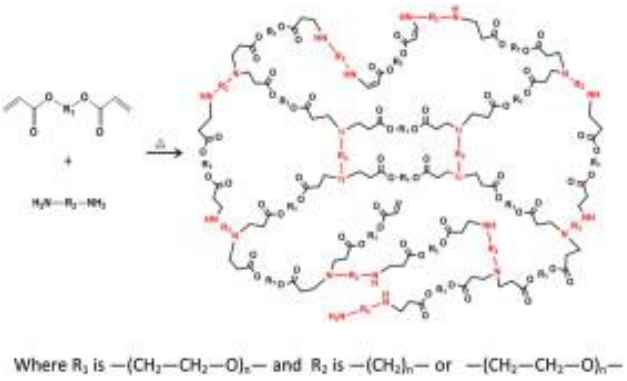

Figure 2.2 Crosslinked PBAE network made with primary diamine and diacrylate.

These networks were synthesized via a facile one-pot Michael's addition between primary amines and acrylates. Additionally, hydrophobic antioxidants, curcumin and quercetin, were also incorporated as comonomers. These networks demonstrate their potential for oxidative stress protection through the controlled release of antioxidants [21-23]. We further functionalized our PBAE systems with disulfide-containing amine, enabling redox-responsive release (Figure 2.3).

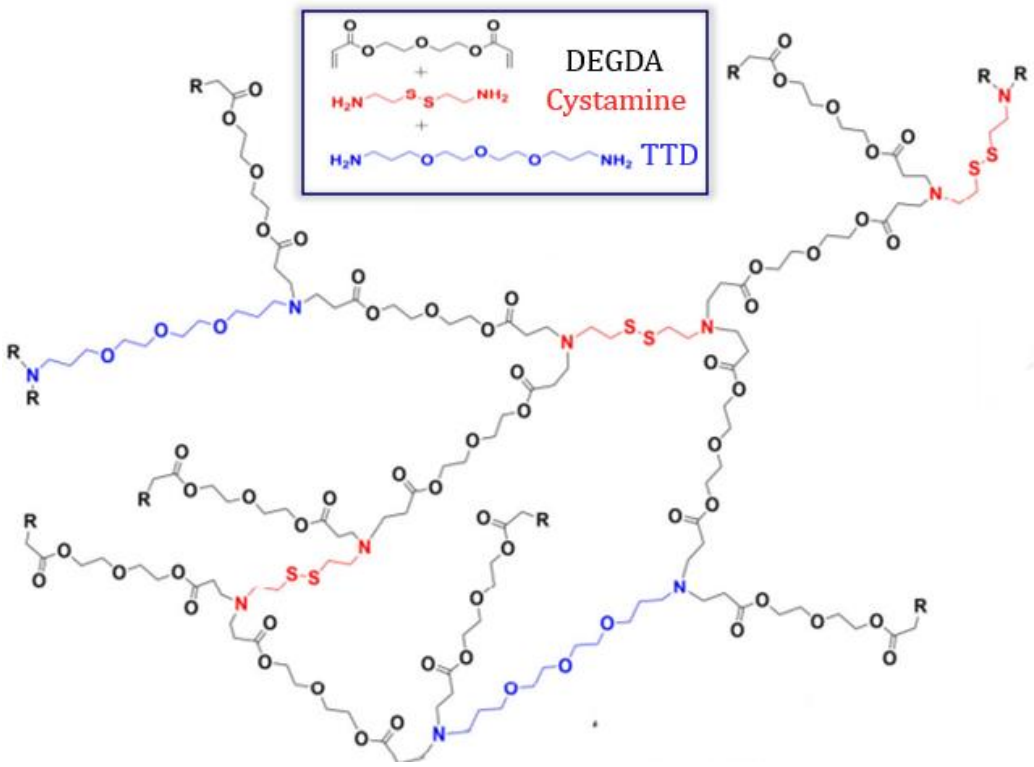

Figure 2.3 Structure of disulfide containing PBAE.

While these disulfide-containing PBAE did not offer antioxidant protection in their disulfide form, their free thiol form significantly mitigated oxidative stress[24]. Despite the promising potential of these disulfide-containing PBAE as redox-responsive polymers, there remains a gap in knowledge regarding the influence of the acrylate monomer on network degradation.

2.3 Development of GSH responsive PBAE networks

Understanding the factors that impact the properties and behavior of polymeric networks is crucial for precise control over them. PBAE networks can be tuned by changing reaction conditions such as concentration and reaction time. Additionally, the properties of the networks can be controlled by varying amines, acrylates, the ratio of total amines to acrylates (RTAA), and further network functionalization. Our group has investigated the

influence of several factors to get better control over the properties of the resulting PBAE networks. Biswal et al. evaluated the impact of the ratio of total acrylates to amines (RTAA) and diamine chemistry on the degradation of PBAE networks made with polyethylene glycol diacrylate (PEG400DA) and amines with varied backbone chemistries, these primary amines included 4,7,10-Trioxa-1,13-tridecane diamine (TTD), 2,2′ (ethylenedioxy) bis ethylamine (EDBE), and Hexamethyldiamine (HMD), (Figure 2.4). The study concluded that the presence of the C-O bonds found on primary diamines increased the hydrophilicity of the resulting networks, leading to increased water absorption by the network and faster degradation. Lower RTAA was also associated with faster degradation due to the excess of primary amines, due to the stronger nucleophilicity of amine groups [23].

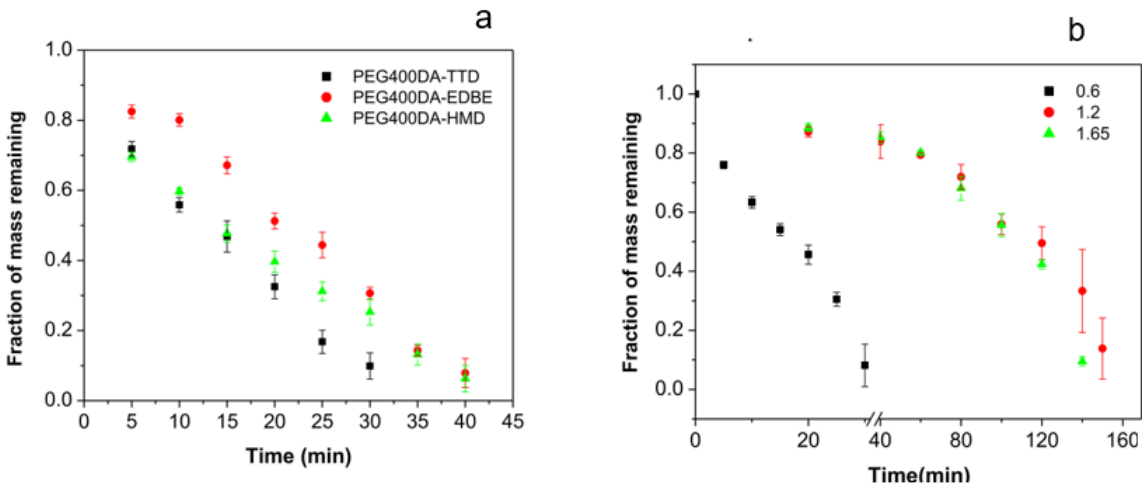

Figure 2.4 Fraction of the mass remaining of the PBAE polymers made with different amines (a), made with TTD, and varied RTAA (b).

In addition, Lakes et al. functionalized these PBAE networks with disulfide bonds by introducing cystamine (CystA). These reducible systems were cleaved in the presence of a reducing agent, 2-mercaptoethanol (Figure 2.5).

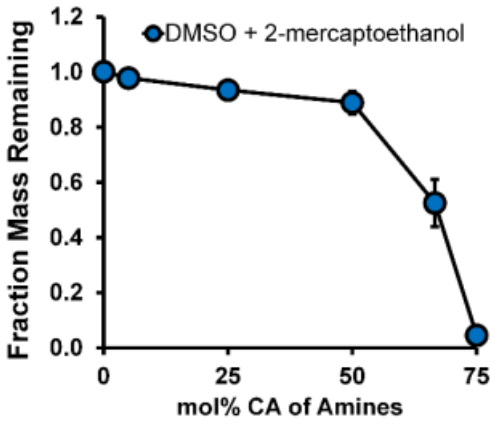

Figure 2.5 Fraction of mass remaining of disulfide containing PBAE following a wash in 2-mercaptoethanol and DMSO.

In this work, we relied on our previous findings to expand the understanding of the swelling and degradation potential of disulfide-containing PBAE systems made with varied acrylates. Our study is summarized as a control panel, with each knob representing a variable we can tune (Figure 2.6). The RTAA was kept at 1, resulting in a balanced network with the highest molecular weight [25, 26]. We varied the ratio of cystamine (CystA) and TTD, acrylate functionality, and concentration of the monomer feed.

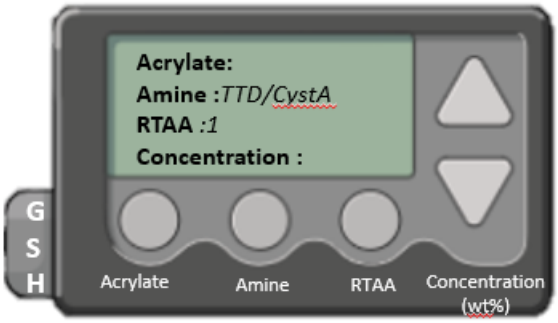

Figure 2.6 Control panel analogy of PBAE systems and controlled variables.

Our current work expanded our understanding of the degradation potential of disulfide containing PBAE systems made with more hydrophilic polyethylene glycol diacrylate, (PEG400DA), more hydrophobic diethylene glycol diacrylate (DEGDA) and varied ratios of diamines, CystA and TTD. The reduction of disulfide bonds, which occurs in the presence of GSH, allows for controlled degradation of the polymers and can be controlled by tailoring the amount of disulfide bonds.

Biomaterial geometry can also be tuned to optimize cytosol delivery. The PBAE systems we have developed have been limited to thin films, which substantially narrows their applicability, particularly for cytosol deliveries. The current work provides a better

understanding of nanogel synthesis limitations while working with diacrylates. Here, we developed disulfide PBAE nanogels by increasing the acrylate functionality of monomer by incorporating a triacrylate (Figure 2.7).

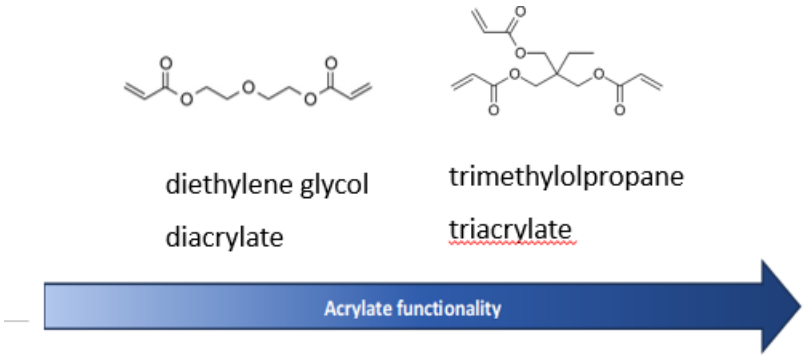

Figure 2.7 Structure of diacrylate and triacrylate used for PBAE synthesis.

Branched triacrylate increases the crosslinking density of the resulting PBAE network, allowing it to form crosslinked systems at lower monomer feed, thus expanding our current hydrogel geometry.

2.4 Project outcomes

In summary, this work provides a better understanding of the impact of acrylate hydrophilicity and disulfide crosslinks on the degradation potential of disulfide-containing PBAE systems in physiological levels of GSH. It also showcases the development of disulfide-containing PBAE nanogels achieved by increasing the acrylate functionality.

CHAPTER 3. THE IMPACT OF ACRYLATE HYDROPHILICITY ON THE DEGRADATION OF DISULFIDE-CONTAINING PBAE THIN FILMS AT PHYSIOLOGICAL GSH LEVELS

3.1 Introduction

Glutathione (GSH) is a tripeptide composed of glutamine, cysteine, and glycine. At concentrations of 1-10mM, GSH is one of the most abundant chemicals found in the cytosol of mammalian cells[6, 7]. In a healthy cell, most glutathione is found in its thiol form, GSH, while the fraction of its disulfide form, GSSG, is roughly 1/100 [27, 28]. GSH is a primary cellular antioxidant that plays a critical role in scavenging reactive oxygen species (ROS) and other free radicals, thereby protecting cellular components from oxidative damage. It regulates cellular redox homeostasis, protecting cells from lipid peroxides, reactive oxygen and nitrogen species, and various xenobiotics[8-11]. Beyond its antioxidant function, GSH participates in redox signaling, enzymatic reactions, and the regulation of cellular processes such as DNA synthesis and repair[29, 30].

There is growing interest in developing GSH-targeted drug delivery therapies, commonly accomplished by incorporating GSH-responsive crosslinkers such as disulfide bonds [31-33]. By incorporating GSH-sensitive linkages into drug delivery systems, researchers can engineer formulations that remain stable in the extracellular environment but undergo rapid cleavage in response to high GSH concentrations. This selective activation mechanism enables the controlled release of therapeutics, maximizing drug efficacy while minimizing systemic toxicity[34, 35]. Additionally, GSH levels can be augmented through a disulfide exchange reaction, resulting in the depletion of cellular antioxidant defense [36, 37]. Our group has previously developed hydrolytically degradable disulfide-containing poly(beta-amino ester) (PBAE) hydrogels with tunable ROS protection. By varying the oxidative

stress of these materials, we were able to increase in the LD50 of the material by an order of magnitude[24].

PBAE polymers have been extensively utilized in the synthesis of hydrogel-based drug delivery systems[23, 38, 39]. PBAE systems are made through Michael's addition between amines and acrylates and have been gaining popularity due to their adaptable chemical compositions and properties, straightforward synthesis methods, and cost-effectiveness. Gupta et al. has successfully synthesized PBAE nanogels to increase the bioavailability of the hydrophobic antioxidant curcumin, allowing for its control release and, consequently, enhanced oxidative stress protection of mitochondria[22]. PBAE scaffolds have also been advantageous by mimicking extracellular matrix and providing structural support for cell attachment and further tissue development. Filipovic et al. developed a 3D scaffold containing a combination of synthetic polymer, poly(2-hydroxyethyl methacrylate) (PHEMA), and a natural polymer, gelatin. The resulting nontoxic scaffolds offered improved cell adhesion compared to control samples[40].

Despite numerous studies of PBAE hydrogel systems, the data on PBAE tunability is still limited. In the present study, we further expanded on the impacts of acrylate hydrophilicity on the swelling and degradation rates of disulfide-containing PBAE systems. Additionally, we assess the impact of cellular GSH levels on the degradation kinetics of these redox-sensitive biomaterials.

3.2 Materials

All reagents were used as received without further purification steps. Cystamine dihydrochloride (CystA), glutathione (GSH), 2-mercaptoethanol (2-ME) were purchased from Thermo Scientific (Waltham, MA), and 1,8-Diazabicyclo(5.4. 0)undec-7-ene (DBU)

was purchased from Sigma Aldrich (Milwaukee, WI). Diethylene glycol diacrylate (DEGDA), polyethylene glycol (400) diacrylate (PEG400DA), and 4,7,10-trioxa-1,13-tridecanediamine (TTD) were purchased from Polysciences Inc. (Warrington, PA). All solvents were purchased from J.T. Baker (Phillipsburg, NJ).

3.3 Methods

3.3.1 PBAE gel synthesis

PBAE gels were synthesized via one -step Michaels's addition between acrylates and diamines. The stoichiometric molar ratio of total acrylates to amine protons was kept at 1, and the total reagent concentration was 45 wt%. First, cystamine was sonicated with DMSO to aid in solubilization. When cystamine was used as only diamine, 75 vol% DMSO and 25vol% DBU were used. Next, TTD was added, followed by acrylate, DEGDA, or PEG400DA. The mixture was then vortexed for 1 minute, dispensed on a Teflon plate, and polymerized for 24 hrs at 60 C. The gels were then washed with DMSO three times to remove any unreacted reagents; next, DMSO was removed by washing the gels twice in acetone. After the acetone wash, gels were air-dried in the fume hood for 1 hr, flash-frozen with nitrogen, and freeze-dried for 24 hrs (−80°C, <0.1 mBar). Dried gels were stored in the freezer with desiccant.

Table 3.1 PBAE gel compositions and their abbreviations

Gel abbreviation	Molar amine percentage composition	
	CystA (mmol %)	**TTD (mmol %)**
0/100 CystA/TTD	0	100
25/75 CystA/TTD	25	75
50/50 CystA/TTD	50	50
100/0 CystA/TTD	100	0

3.3.2 PBAE degradation

Degradation of PBAE gels was carried out in various concentrations of GSH at 37°C. To determine the impact of cellular levels of glutathione on the gel degradation, gels were incubated In 0, 1, 10, and 20 mM GSH/PBS at pH 7.4. Dried gels were cut into circular disks, weighted, and incubated in desired media, under sink conditions. Samples were stored in a water bath shaker at 70 rpm at 37 °C. At desired time points, samples were removed, swollen gels were dried with a kimwipe and weighted. To maintain sink conditions, the media was replaced every 24 hrs. The weight swelling ratio (q) was calculated as a ratio of swollen gel mass (Ws) and initial mass (W_0). To determine the fraction of the mass remaining, gels were removed from the media, and dried under the vacuum to remove residual media. The fraction of the mass remaining was calculated as a ratio of final dry mass (W_d) and initial mass (W_0).

$$q = \frac{W_s}{W_o} \quad (1)$$

$$Fraction\ of\ mass\ remaining = \frac{W_d}{W_o} \quad (2)$$

3.4 Results

3.4.1 DEGDA gels

To assess the effect of physiological levels of glutathione on disulfide-containing PBAE systems, we used DEGDA-based gels with varying CystA/TTD ratios. Our findings revealed a significant increase in degradation time at higher cystamine ratios (Figure 3.1). The responsiveness of these gels to GSH was evaluated by incubating them in varied concentrations of GSH/PBS. Degradation time significantly decreased in gels exposed to 10 and 20 mM GSH/PBS. The gel degradation acceleration and swelling rate increase in samples incubated in GSH was comparable to those in 2-ME. Gels with 25/75 and 50/50 CystA/TTD ratios showed increased swelling ratios and decreased degradation time at 10 and 20 mM GSH/PBS, while no significant difference was observed at 1 mM GSH/ PBS. Interestingly, gels composed entirely of cystamine (100/0 CystA/TTD) exhibited an insignificant increase in swelling at 10 and 20 mM, but their degradation times remained unchanged. Gels containing no cystamine (0/100 CystA/TTD) showed no correlation in their swelling or degradation trends at varied GSH concentrations (Figure 3.2).

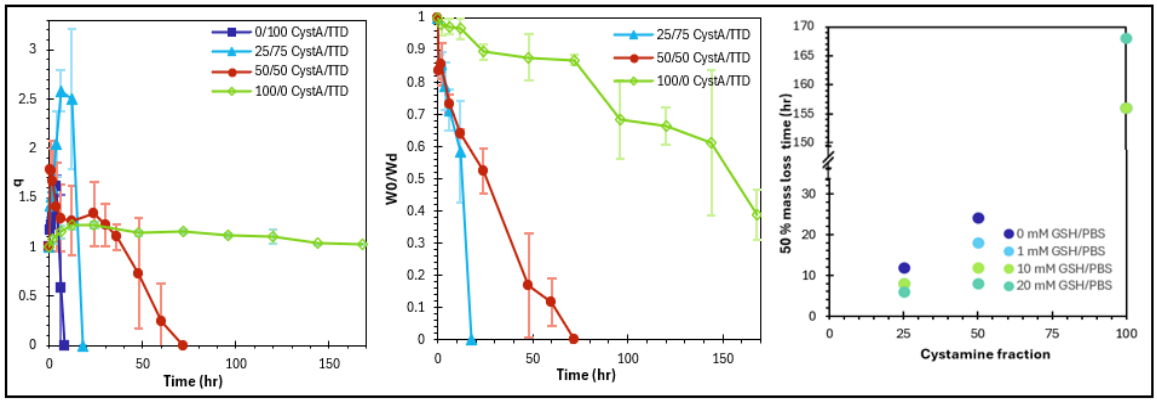

Figure 3.1 Swelling rates, fraction of mass remaining, the degradation time of DEGDA gels with varied cystamine content in 0mM GSH/PBS (left to right). N=3, error bars: std. dev.

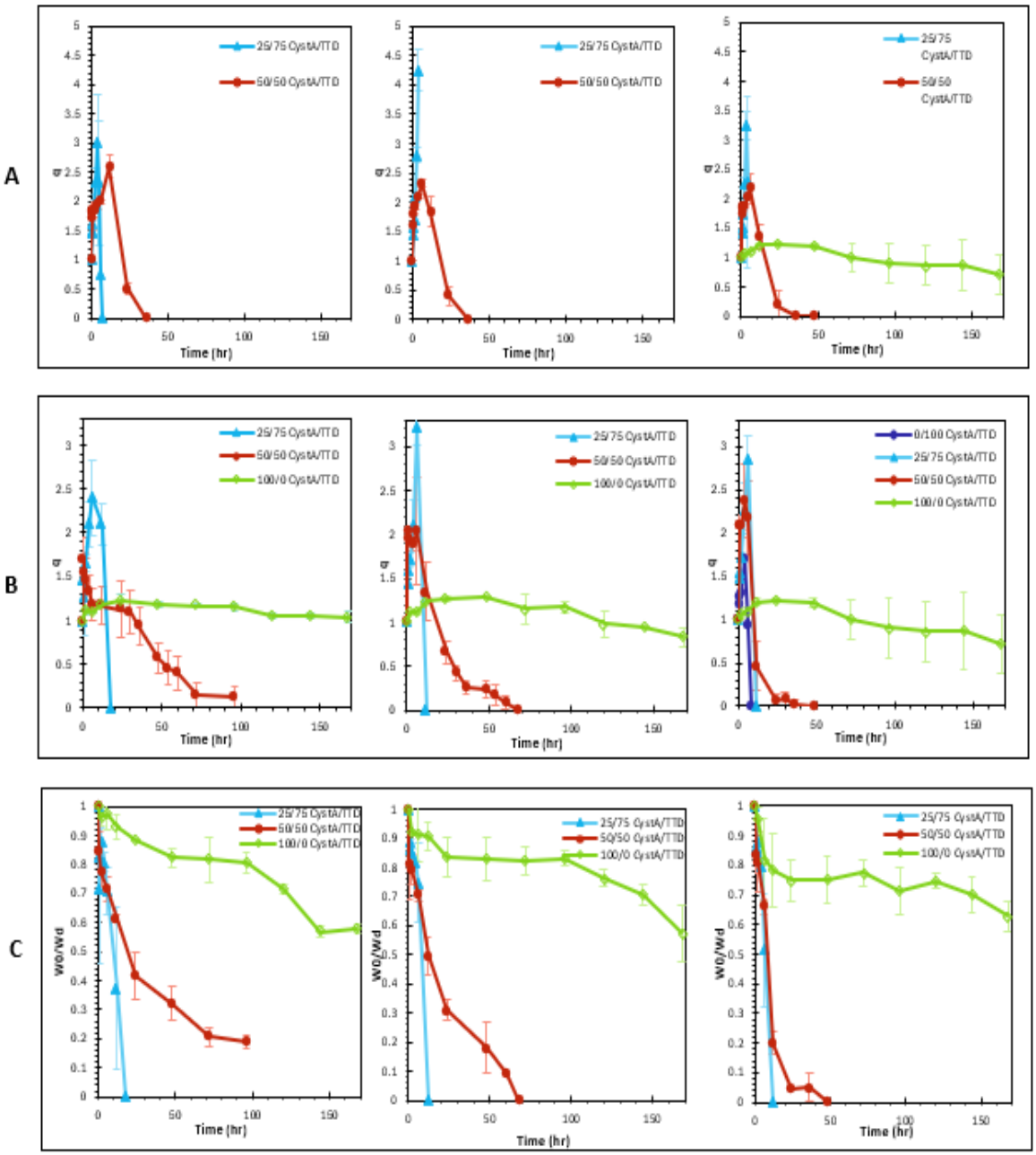

Figure 3.2 **A**: swelling rates of DEGDA gels with varied cystamine content in 1, 10, 20 mM 2-ME/PBS (left to right); **B**: swelling rates of DEGDA gels with varied cystamine content in 1, 10, 20 mM GSH/PBS (left to right); **C**: fraction of mass remaining rates of DEGDA gels with varied cystamine content in 1, 10, 20 mM GSH/PBS (left to right). N=3, error bars: std. dev.

Since no significant swelling was observed for 100/0 CystA/TTD samples in PBS, GSH/PBS, or 2-ME/PBS we evaluated the swelling ratios in non-aqueous media. The swelling ratio of DEGDA gels containing 100/0 CystA/TTD was also evaluated in 2-ME/DMSO, 2-ME/PBS, and DMSO for 24 hrs to assess the ability of the gels to be reduced and investigate the impact the media on the reduction of these disulfide containing systems. There was a notable increase in swelling and complete degradation of samples incubated in 2-ME/DMSO. Samples incubated in DMSO demonstrated increased swelling compared to samples in PBS, both with and without 2-ME, but did not degrade.

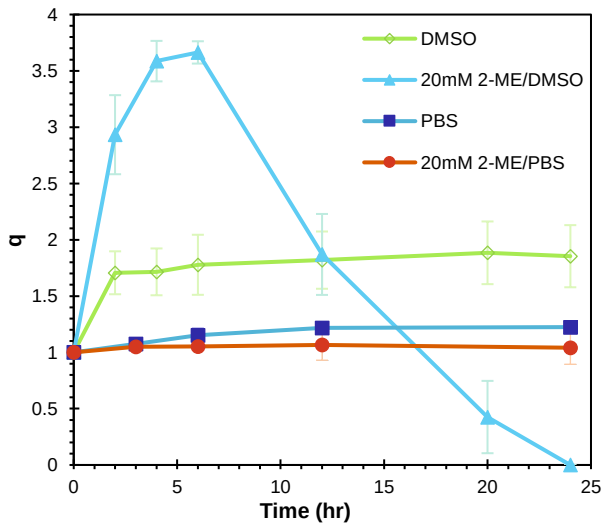

Figure 3.3 Swelling rates of 100/0 CystA/TTD DEGDA gels in PBS, DMSO, 20 mM 2-ME/PBS, 20 mM 2-ME/DMSO. N=3, error bars: std. dev.

3.4.2 PEG400DA gels

Gels with PEG400DA and varied ratios of CystA/TTD were developed to investigate the impact of acrylate hydrophilicity on the degradation and swelling rates. Both 25/75 and

50/50 CystA/TTD gels were evaluated in varied GSH concentrations. Similarly to gels made with DEGDA, these systems exhibited increased degradation time at higher cystamine ratios. Faster degradation rates were also observed at 10 and 20 mM GSH/PBS, with 25/75 and 50/50 fully degrading within 6 and 12 hrs, respectively. Samples containing 50/50 CystA/TTD also demonstrated increased swelling rates at 10 and 20 mM GSH/PBS, while no significant difference in swelling rates was observed in 25/75 CystA/TTD gels.

Figure 3.4 Swelling rates, fraction of mass remaining, the degradation time of PEG400DA

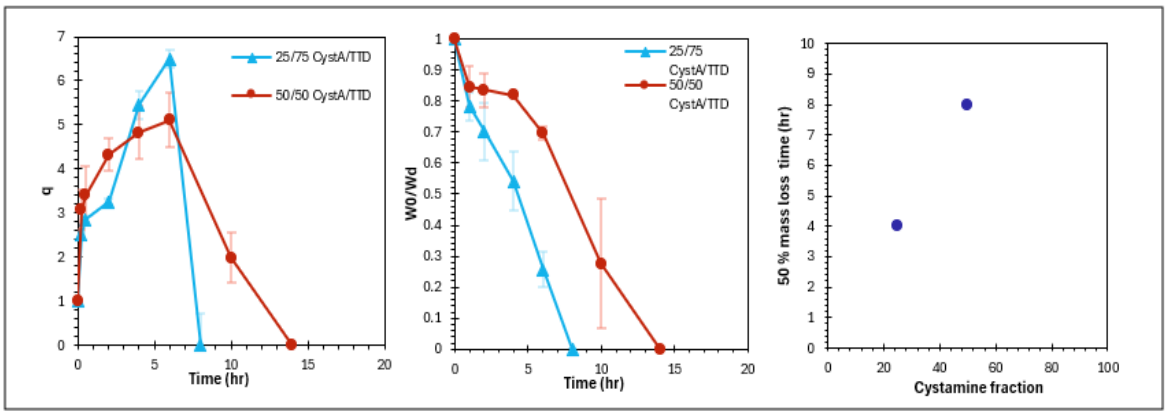

gels with varied cystamine content in 0mM GSH/PBS (left to right). N=3, error bars: std. dev.

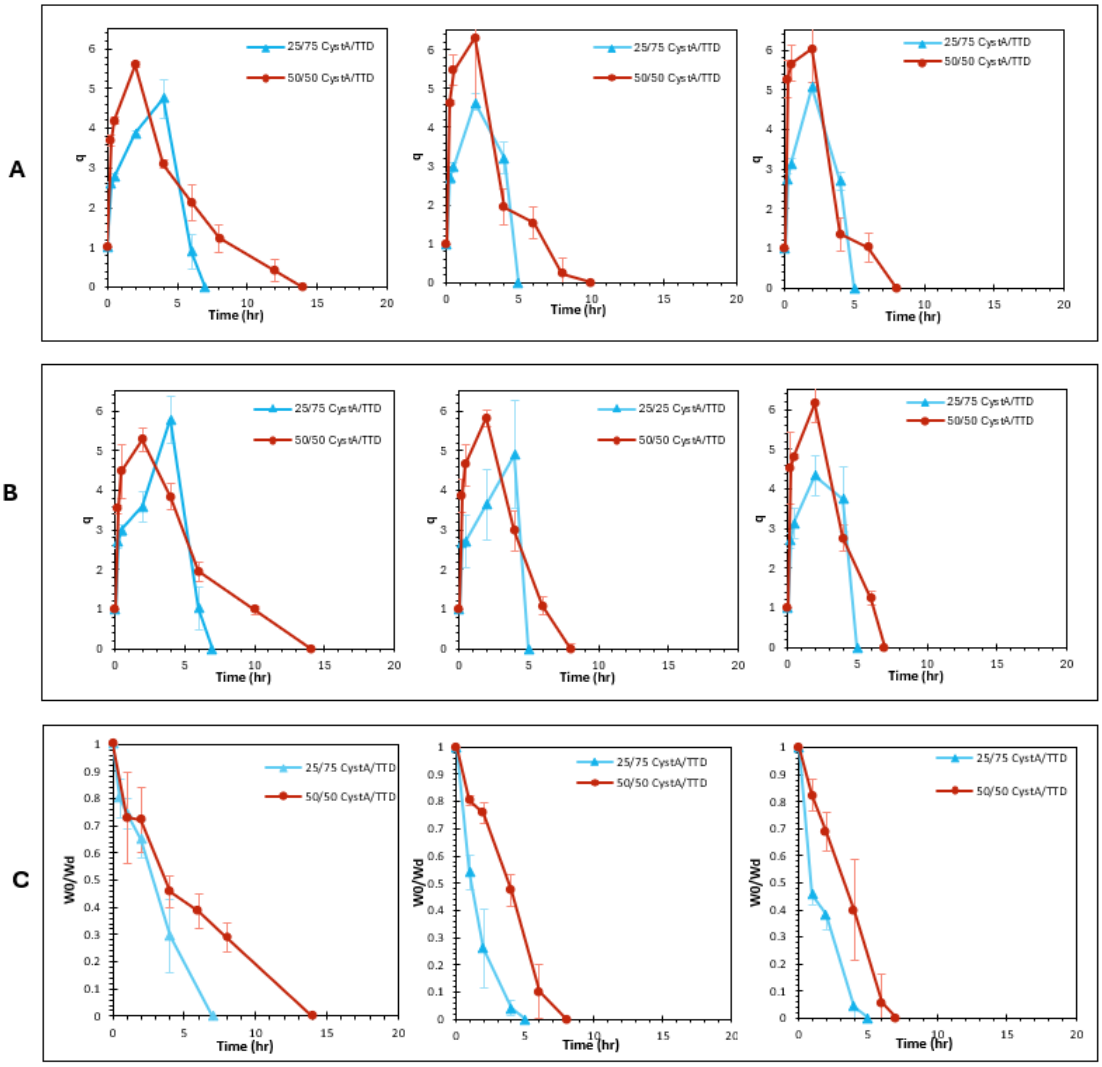

Figure 3.5 **A**: swelling rates of PEG400DA gels with varied cystamine content in 1, 10, 20 mM 2-ME/PBS (left to right); **B**: swelling rates of PEG400DA gels with varied cystamine content in 1, 10, 20 mM GSH/PBS (left to right); **C**: fraction of mass remaining rates of PEG400DA gels with varied cystamine content in 1, 10, 20 mM GSH/PBS (left to right). N=3, error bars: std. dev.

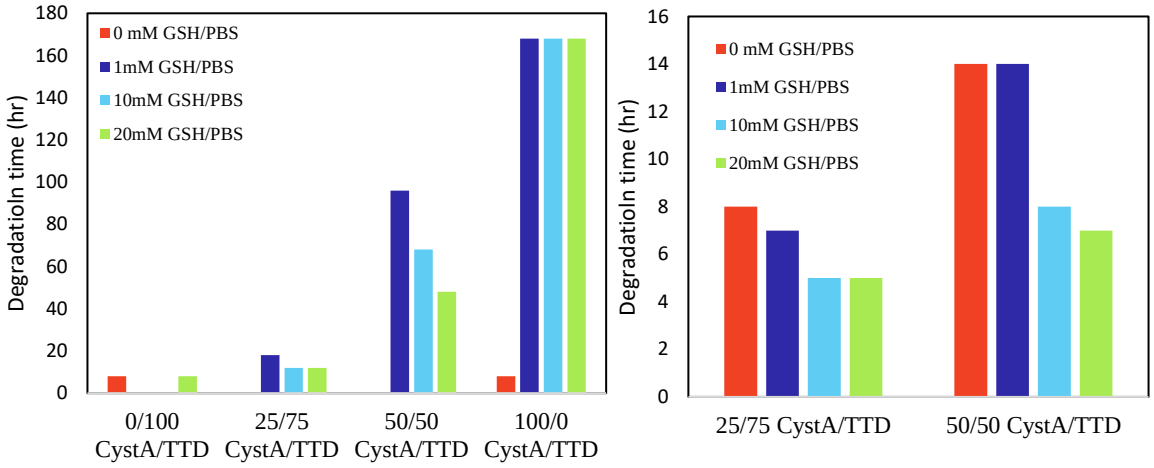

Figure 3.6: Degradation time of DEGDA gels made with 0/100, 25/75, 50/50, 100/0 CystA/TTD (**A**), and PEG400DA gels made with 25/75 and 50/50 CystA/TTD in 0, 1, 10, 20 mM GSH/PBS(**B**). N=3, error bars: std. dev.

Overall, degradation time gradually increased as the fraction of CystA increased, which was observed for gels made with either DEGDA or PEG400DA (Figure 3). A notable decrease in degradation time was observed for 25/75 and 50/50 gels made with either DEGDA or PEG400DA incubated in 10 and 20 mM GSH/PBS.

3.5 Discussion

3.5.1 Incorporation of PEG400DA into PBAE networks increased swelling and degradation of the resulting gels

Previously, we developed disulfide-containing PBAE systems using DEGDA as our acrylate containing monomer. In this study, we synthesized disulfide-containing PBAE gels with a more hydrophilic acrylate, PEG400DA. We investigated the impact of diacrylate hydrophilicity on the swelling and degradation potential of disulfide-containing PBAE systems. As anticipated, degradation times were shorter for gels made with PEG400DA, while the swelling rates were significantly higher than those made with DEGDA. Swelling

rates are impacted by both hydrophilicity of the polymer and chain elasticity. The highest swelling rates for gels containing 0/100 and 25/75 CystA/TTD were noted shortly before gel degradation. In addition, 25/75 CystA/TTD gels made with PEG400DA had a nearly three times greater swelling rate observed shortly before the gel's complete degradation. The increased swelling potential of PEG400DA gels is possibly due to the higher elasticity, increased hydrophilicity, and crosslinking density of PEG400DA compared to DEGDA. These findings align with published research; for example, Rekowsa et al. had previously reported an increase in tensile strength and elongation at the break of hydrogels made with higher molecular weights of PEGDA[41].

3.5.2 Swelling and degradation rates decrease as the fraction of CystA in PBAE networks increased

Incorporating disulfide bonds also significantly impacted the swelling and degradation rates of our PBAE systems. Slower degradation times were observed as the fraction of CystA increased (Figure 1A). Additionally, 50/50 and 100/0 CystA/TTD gels had significantly lower swelling rates than 0/100 and 25/75 CystA/TTD gels. Unlike hydrolytically degradable ester and ether bonds of this PBAE network, disulfide bonds do not undergo hydrolysis and are only broken via bond reduction. Due to the more hydrophobic nature of DEGDA, we hypothesize that limited degradation of 100/0 CystA/TTD systems can limit the reduction of disulfide bonds when the reducing agent is in PBS. To evaluate this claim, these gels were incubated in 20mM 2-ME in polar solvent, DMSO, and the swelling rates of these samples were monitored for 24 hrs. Samples in DMSO (without 2-ME) were used as a negative control. Gels incubated in 20mM 2-ME/DMSO had significantly higher swelling rates and degraded completely within 24 hrs compared to samples incubated in PBS, DMSO, 20mM 2-ME/DMSO , and 20mM 2-

ME/PBS, which suggests that these networks are reducible in non-aqueous media. Due to the more hydrophobic entire of DEGDA, 2-ME likely has very limited accessibility to its disulfide bonds. Polar and aprotic DMSO decreases hydrophobic interactions within the polymer, enabling 2-ME to reduce its disulfide bonds.

3.5.3 100/0 CystA/TTD PBAE systems did not respond to elevated GSH concentrations

Increased degradation rates in 10 and 20 mM GSH/PBS were observed for 25/75 and 50/50 CystA/TTD gels made with both DEGDA and PEG400DA, which was likely caused by the reduction of disulfide bonds by thiolated GSH. However, there was limited degradation for 100/0 CystA/TTD gels made with DEGDA, likely due to the limited accessibility of the reducing agent.

3.6 Conclusion

It was found that disulfide-containing PBAE gels made by one-step Michaels addition using more hydrophilic acrylate, PEG400DA, had larger swelling ratios and faster degradation rates compared to disulfide-containing PBAE systems made with DEGDA. Further, the incorporation of disulfide bonds resulted in increased degradation times of PBAE gels. This held true for gels made with either DEGDA or PEG400DA. Resulting disulfide containing PBAE networks showed a concentration-dependant increase in their swelling ratios and decrease in their degradation times at near physiological levels of GSH, 10 and 20 mM.

CHAPTER 4. THE IMPACT OF ACRYLATE FUNCTIONALITY ON THE DEGRADATION OF DISULFIDE-CONTAINING PBAE THIN FILMS AT PHYSIOLOGICAL GSH LEVELS.

4.1 Introduction

Implantable biomaterials have been extensively utilized for structural support, cell encapsulation, and therapeutic deliveries[42]. For many of these intended applications, the biomaterial's overall mechanical properties and its ability to degrade (either enzymatically or hydrolytically) in a controlled fashion are extremely important[43]. PBAE polymers' inherent biocompatibility, facile synthesis, and tunable degradation profiles made them an attractive candidate for implantation medicine and beyond[17].

The properties and structure of acrylate monomers are crucial in determining the polymer’s mechanical properties, swelling, and degradation rate. Brey et al. employed linear diacrylate, 1,6-hexanediol ethoxylate diacrylate, and branched pentaerythritol triacrylate monomers to control mechanical properties. The study concluded that increasing the branched monomer fraction resulted in increased compressive modulus [44].

Here, we examine the impact of the acrylate functionality of monomers on the degradation of disulfide-containing PBAE systems and further investigate this behavior in the physiological levels of GSH.

4.2. Materials

All reagents were used as received without further purification steps. Cystamine dihydrochloride (CystA), glutathione (GSH), trimethylolpropane (TMPTA) were purchased from Thermo Scientific (Waltham, MA). Polyethylene glycol (400) diacrylate (PEG400DA), and 4,7,10-trioxa-1,13-tridecanediamine (TTD) were purchased from

Polysciences Inc. (Warrington, PA). All solvents were purchased from J.T. Baker (Phillipsburg, NJ).

4.3 Methods

4.3.1 PBAE gel synthesis

PBAE gels were synthesized via one-step Michaels's addition between acrylates and amine monomers. The stoichiometric molar ratio of total acrylates to amines was kept at 1, and the total reagent concentration was 45 wt%. First, cystamine was sonicated with DMSO to aid in solubilization. Next, TTD was added, followed by the acrylate, TMPTA, PEG400DA, or both. The mixture was then vortexed for 1 minute, dispensed on a Teflon plate, and polymerized for 24 hrs at 60 C. The gels were then washed with DMSO three times to remove any unreacted reagents; next, DMSO was removed by washing the gels twice in acetone. After the acetone wash, gels were air-dried in the fume hood for 1 hr, flash-frozen with nitrogen, and freeze-dried for 24 hrs (−80°C, <0.1 mBar). Dried gels were stored in the freezer with desiccant.

Table 4.2 PBAE gel compositions and their abbreviations

Gel abbreviation	Molar amine percentage composition	
	CystA (mmol %)	**TTD (mmol %)**
0/100 CystA/TTD	0	100
25/75 CystA/TTD	25	75
50/50 CystA/TTD	50	50

4.3.2 PBAE degradation

Degradation of PBAE gels was carried out in various concentrations of GSH at 37°C. To determine the impact of cellular levels of glutathione on the gel degradation, gels were incubated In 0, 1, 10, and 20 mM GSH/PBS at pH 7.4. Dried gels were cut into circular disks, weighted, and incubated in desired media, under sink conditions. Samples were stored in a water bath shaker at 70 rpm at 37 C. At desired time points, samples were removed, swollen gels were dried with a kimwipe and weighted. To maintain sink conditions, the media was replaced every 24 hrs. The swelling ratio (q) was calculated as a ratio of swollen gel mass (W_s) and initial mass (W_0).

$$q = \frac{W_s}{W_o} \quad (1)$$

4.4 Results

4.4.1 Degradation of TMPTA gels

The degradation potential of 0/100, 25/75, and 50/50 CystA/TTD TMPTA gels was evaluated by measuring the equilibrium swelling ratio as a function of GSH concentration. During the initial 2 hrs, all gels reached their maximum swelling potential. No gel degradation was observed during 120 hrs of monitoring. Interestingly, increased GSH concentration had no impact on swelling ratios of TMPTA gels.

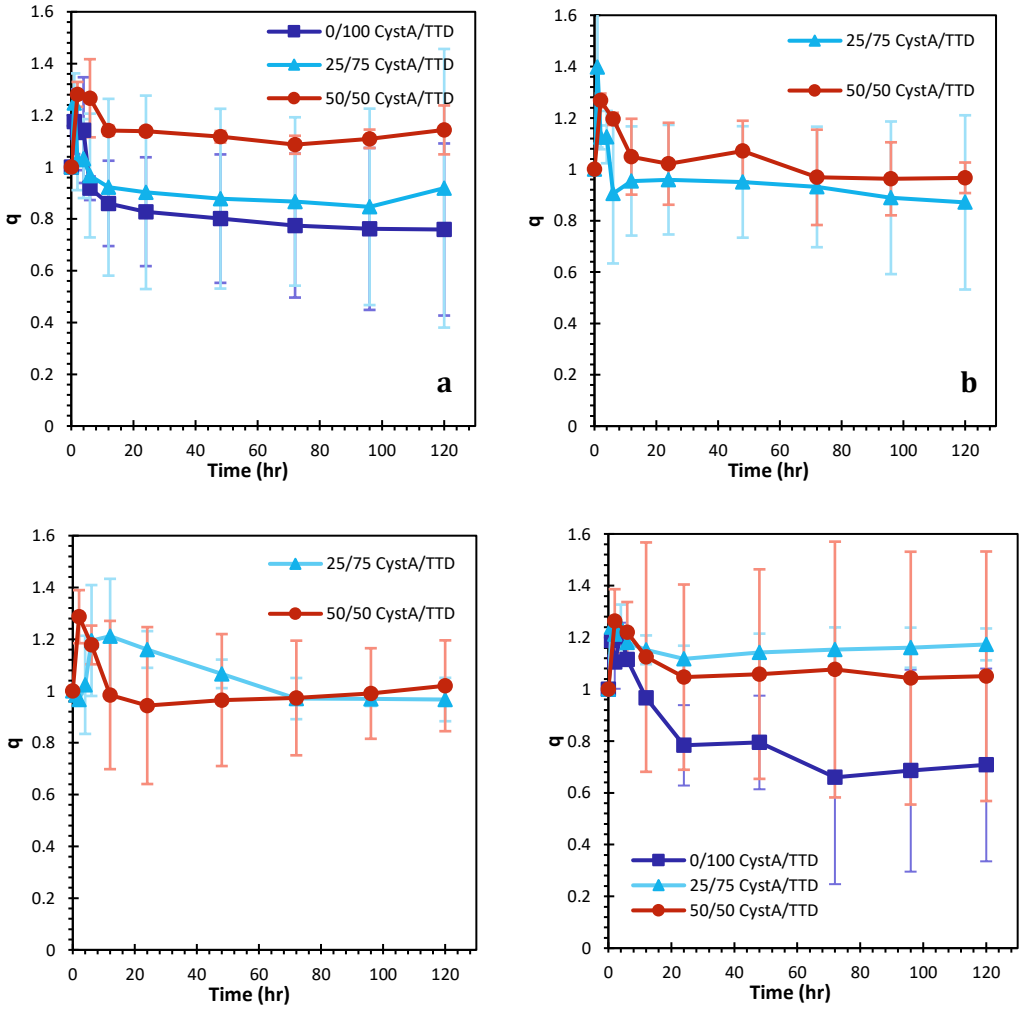

Figure 4.1 Swelling ratios of TMPTA gels with varied cystamine content in 0mM (a), 1 mM (b), 10 mM (c), 20 mM (d) GSH in PBS. N=3, error bars: std. dev.

4.4.2 Degradation of TMPTA gels 0/100 CystA/TTD gels with varied ratios of TMPTA/PEG400DA

Varied amounts of PEG400DA were introduced to mitigate the non-swelling and non-degrading profiles of PBAE gels with TMPTA only. PBAE networks' degradation time with varied ratios of TMPTA/PEG400DA ranged from 2 to 96 hrs. Gels containing 20/80 TMPTA/PEG400DA were fully degraded within 2 hrs, while gels with the highest TMPTA content, 90/10 TMPTA/PEG400DA degraded within 96 hrs.

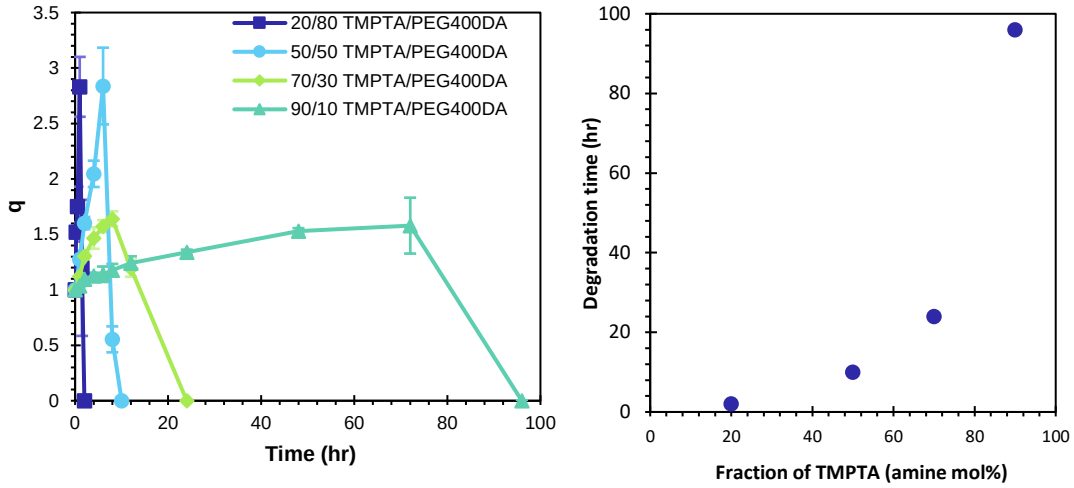

Figure 4.2 Swelling ratios (a), degradation time(b) of 0/100 CystA/TTD gels with varied ratios of TMPTA/PEG400DA. N=3, error bars: std. dev.

4.4.2 Degradation of 70/30 TMPTA/PEG400DA gels

To investigate the impact of disulfide bonds on the swelling and degradation profile of PBAE systems in varied amounts of GSH/PBS, 70/30 TMPTA/PEG400DA gels were prepared with 25/75 and 50/50 CystA/TTD. Gels made with 25/75 CystA/TTD degraded within 72 to 120 hrs, with faster degradation time corresponding to samples incubated in 10 and 20 mM GSH/PBS, respectively. Unlike 25/75 CystA/TTD gels, 50/50 CystA/TTD gels did not demonstrate GSH responsiveness, with no notable increase in swelling or degradation during 120 hrs of gel monitoring.

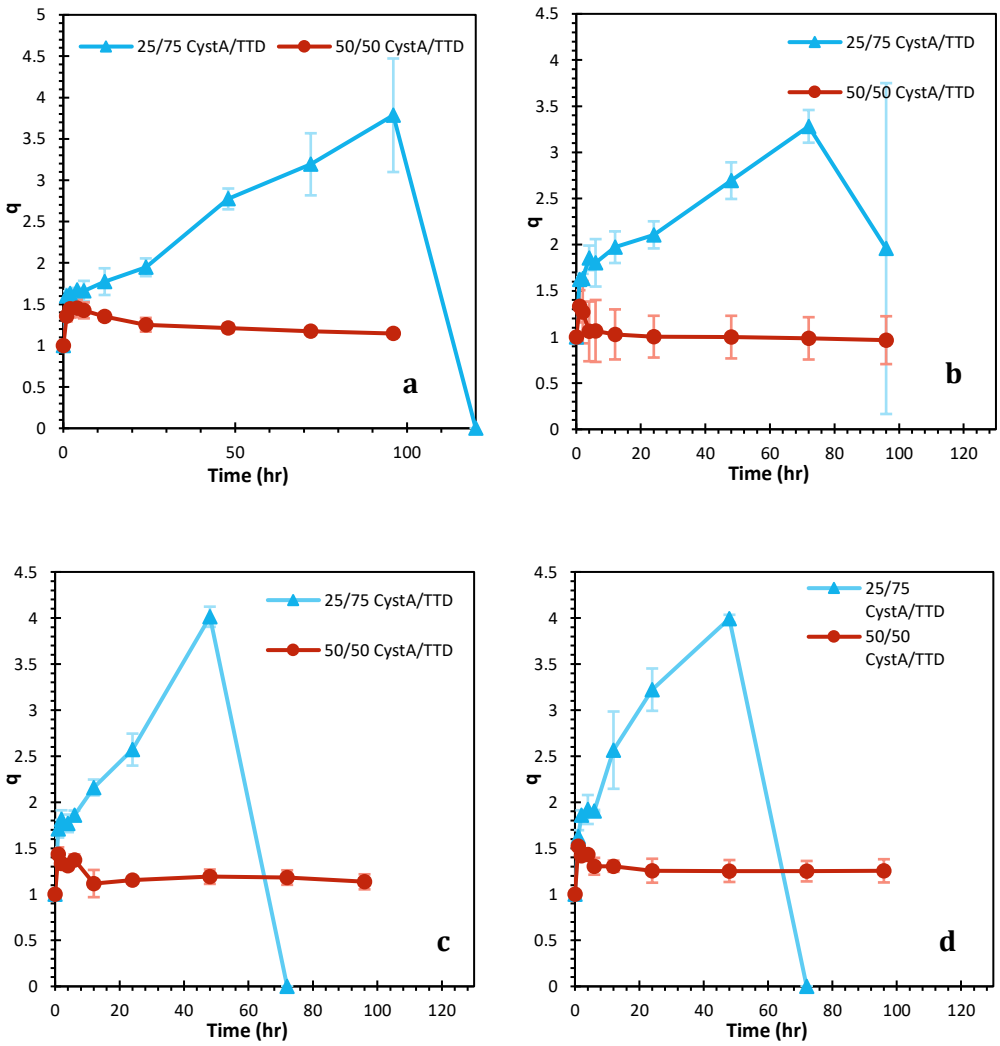

Figure 4.3 Swelling ratios of TMPTA gels with varied cystamine content in 0 mM (a), 1 mM (b), 10 mM (c), and 20 mM (d) GSH in PBS. N=3, error bars: std. dev.

4.4. Discussion

4.4.1 TMPTA-based disulfide-containing PBAE gels do respond to physiological levels of GSH

The acrylate functionality of monomer impacts the crosslinking density of PBAE thin films. Using monomers with higher acrylates leads to a more densely crosslinked network, which generally results in slower degradation rates[45, 46]. Densely crosslinked networks have lower swelling ratios [47, 48]. Additionally, more hydrophobic monomers

lead to the formation of networks where hydrolysis has limited potential, resulting in a non-degrading network. In addition, the denser network may provide less free space for GSH to penetrate and react with the disulfide bonds in the polymer matrix, significantly impairing GSH's reducing potential. As a result, no significant impact on swelling rates and degradation time was observed at increased GSH concentrations. The reduction can be performed in non-aqueous media, such as DMSO or ethanol, to assess if disulfide bonds can be reduced when hydrophobic polymer interactions decrease.

4.4.2 Incorporation of PEG400DA increases degree of swelling and accelerates degradation

To enhance the non-degrading and non-swelling profiles of TMPTA-based PBAE systems, varied ratios of PEG400DA were used to increase the hydrophilicity of the resulting networks. PEG monomers have been extensively used to increase the affinity of water in hydrogel networks[49, 50]. PEG400Da provided multiple water binding sites, thus increasing the degree of swelling of PEG400DA/TPTA systems. Additionally, incorporating PEG400DA decreases the crosslinking density of the PBAE networks by decreasing the acrylate functionality of monomers [51, 52]. Decreased crosslinking density and increased hydrophilicity of these PBAE polymers resulted in accelerated degradation time by promoting hydrolysis of the networks.

4.4.3 Disulfide-containing PBAE gels made TMPTA/PEG400DA have higher swelling and degradation rates in physiological levels of GSH.

To further tailor GSH responsiveness, CystA content was increased in the PBAE network made with 70/30 TMPTA/PEG and evaluated the swelling degradation behavior of these gels in physiological levels of GSH. Similarly to DEGDA-based PBAE networks, 25/75 CystA/TTD gels showed a prominent response to the increased GSH concentrations,

with increased swelling ratios and accelerated network degradation at higher GSH concentrations. On the contrary, no impact of GSH levels was noted in 50/50 CystA/TTD systems, proving them to be less responsive than 50/50 CystA/TTD gels made with DEGDA. The perceived lack of GSH responsiveness could be attributed to the nonsignificant swelling increase due to hydrogen bond formation. Limited rotation of disulfide bonds offers a more rigid network resulting in induced hydrogel bonding between unbound amine protons and double-bonded oxygen of the carbonyl group [53].

4.5 Conclusion

Increased acrylate functionality can tune the swelling and degradation rates of disulfide-containing PBAE networks. Incorporating more hydrophobic TMPTA significantly increases the degradation time of the resulting PBAE networks, which can be further adjusted by adding more hydrophilic acrylate like PEG400DA.

CHAPTER 5. DEVELOPMENT OF DISULFIDE-CONTAINING PBAE NANOGELS WITH INCREASED ACRYLATE FUNCTIONALITY

5.1 Introduction

The complexity of therapeutic delivery design can equate to the challenges of therapeutic development itself. Drug delivery mechanisms are individually designed to overcome specific delivery challenges to accommodate the desired regimens while maintaining high efficacy. Nano-sized vesicles such as nanoparticles and nanogels have been at the forefront of therapeutic deliveries due to their unique ability to penetrate and retain within cell networks.

Size constraints are crucial for effective cellular uptake and function. Various studies have concluded that the highest endocytosis rates can be achieved with less than 100 nm nanoparticles[54-56]. Further, particles with smaller sizes generally have longer cellular retention times. Aldayel et al. found that 2-10 nm nanoparticles had longer retention time and larger distribution in the inflamed site compared to 100-200 nm nanoparticles[57]. In another study comparing 24 and 37 nm particles, the former had significantly longer retention times, 10 min and 4 hrs after injection[58].

Nanogels and nanoparticles have been extensively used for drug delivery applications. Their small size and large surface area increase the bioavailability of the conjugated drug[59]. Moreover, nanoparticles have been shown to cross the brain barrier, absorb through the endothelial level of the skin, and enter the pulmonary system [60, 61].

Additionally, there is a growing interest in functionalizing biomaterials to achieve targeted release. Extensive research has been done in developing stimuli-responsive nanogels and

nanoparticles that are responsive to changes in pH, light, temperature, and the cell's redox state[62]. Nonetheless, only a fraction of these are FDA-approved, suggesting that further research in this area is necessary[63].

Our group has previously developed PBAE biomaterial that has the potential to respond to changes in the oxidative state of the cell[24]We further investigated its responsiveness to cellular levels of GSH, which resulted in increased swelling and accelerated degradation rates. In this work, we aim to utilize our understanding of the impacts of acrylate hydrophilicity and functionality to develop disulfide-containing PBAE nanogels, which could be further used for redox-responsive cellular delivery.

5.2 Materials

All reagents were used as received without further purification steps. Cystamine dihydrochloride (CystA), glutathione (GSH), trimethylolpropane (TMPTA) were purchased from Thermo Scientific (Waltham, MA). Polyethylene glycol (400) diacrylate (PEG400DA), diethylene glycol diacrylate (DEGDA), and 4,7,10-trioxa-1,13-tridecanediamine (TTD) were purchased from Polysciences Inc. (Warrington, PA). All solvents were purchased from J.T. Baker (Phillipsburg, NJ).

5.3 Methods

5.3.1 DEGDA/TTD gel synthesis

PBAE networks were synthesized via one-pot Michaels addition in acetonitrile (ACN) using DEGDA as an acrylate source and TTD as an amine source. The ratio of total acrylates to amine protons was kept at 1, while the total wt % of monomer feed (DEGDA and TTD) varied from 45 to 1 wt %. DEGDA and TTD were dissolved in ACN,

5.3.2 Sol-gel inversion test

Sample gelation was evaluated after 24 hrs of polymerization at 60 C. The vials containing varied wt % of monomer feed were inverted to investigate whether the solutions had gelated or remained a solution.

5.3.3 The degree of polymerization of 5 wt % DEGDA/TTD solution

The polymerization 5wt % DEGDA/TTD solution was monitored for 48 hrs. The % TTD/DEGDA monomer solution was incubated at 60 C in a 7 ml glass vial. The solution was removed at predetermined time points, and the desired sample amount was diluted in fresh ACN. To assess possible DEGDA consumption by side reactions, DEGDA was incubated in ACN and monitored continuously. The solutions were filtered into HPLC vials using a syringe filter (0.02um Whatman Anapor 10). Samples were analyzed by HPLC, using C18 column, 80 % DI water, 20% ACN, 0.13 % Phosphoric acid as a mobile phase, 1 ml/min flow rate, and isocratic elusion at 40C. The amount of unreacted DEGDA was quantified using a calibration curve.

5.3.4 Curcumin multiacrylate (CMA)/CystA nanogel synthesis

CMA nanogels with varied ratios of CystA/TTD were prepared via one pot Michael's addition in ACN. First, cystamine dihydrochloride was neutralized as follows. CystA was dissolved in 1 N NaOH, triturated with isopropanol, and filtered. The solvent was evaporated, and the precipitate was redissolved in ACN and filtered. CMA was synthesized as previously described. To prepare CMA nanogels, CMA, TTD, and CystA were mixed in ACN, vortexed for 30 s, and polymerized for 24 hrs at 60 C. The RTAA was kept at 1, while the molar ratio of amines, TTD/CystA, was varied.

5.3.5 TMPTA/PEG400DA nanogel synthesis

Nanogels with varied TMPTA and PEG400DA ratios were prepared via one-pot Michaels addition in ACN with varied ratios of CystA/TTD. Monomers were added to a glass vial, mixed, vortexed for 30 s, and polymerized at 60 C.

5.3.6 DLS size measurement

Once polymerized, samples were diluted to 0.1 vol% with fresh ACN and transferred to a glass cuvette. The size of the resulting nanogels was determined by DLS.

5.4 Results

5.4.1 DEGDA/TTD gels with varied monomer wt%

DEGDA/TTD solutions with varied monomer feed, 45, 30, 20, 10, 5, and 1 wt %, were analyzed following 24 hrs of polymerization. The vials were inverted to determine whether the gelation had occurred. Samples containing 10 or more wt% gelated, while samples containing 5 and 1 wt% remained a solution with no other visual changes noted.

Figure 5.1 DEGDA/TTD gels with 45, 30, 20, 10, 5 and 1 monomer feed wt% (left to right).

5.4.2 The degree of polymerization of 5 wt % DEGDA/TTD solution

The 5 wt% DEGDA/TTD solution polymerization was monitored by measuring the fraction of unreacted DEGDA monomer. The DEGDA solution, without TTD, was used as a control. After the initial 6 hrs of reaction, about 10 % of the initial monomer remained, while after 24 hrs of monitoring, less than 2 % of the monomer was present. No loss of DEGDA was noted for control samples.

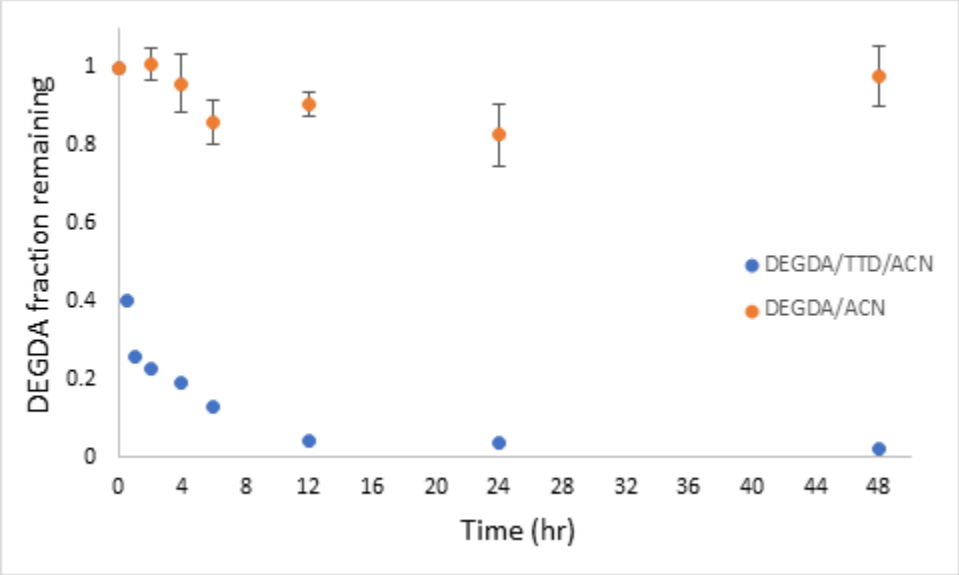

Figure 5.2 The fraction of DEGDA remaining in 5 wt % solution. N=3, error bars: std. dev.

5.4.3 CMA/CystA nanogel synthesis

Once polymerized, CMA nanogels with varied amounts of CystA/TTD were diluted to 0.1 vol% with fresh ACN and analyzed via DLS. Nanogels made with 10/90 CystA/TTD were smaller than other samples, averaging 490 nm, while 0/100 and 25/75 samples were around 700 and 800 nm.

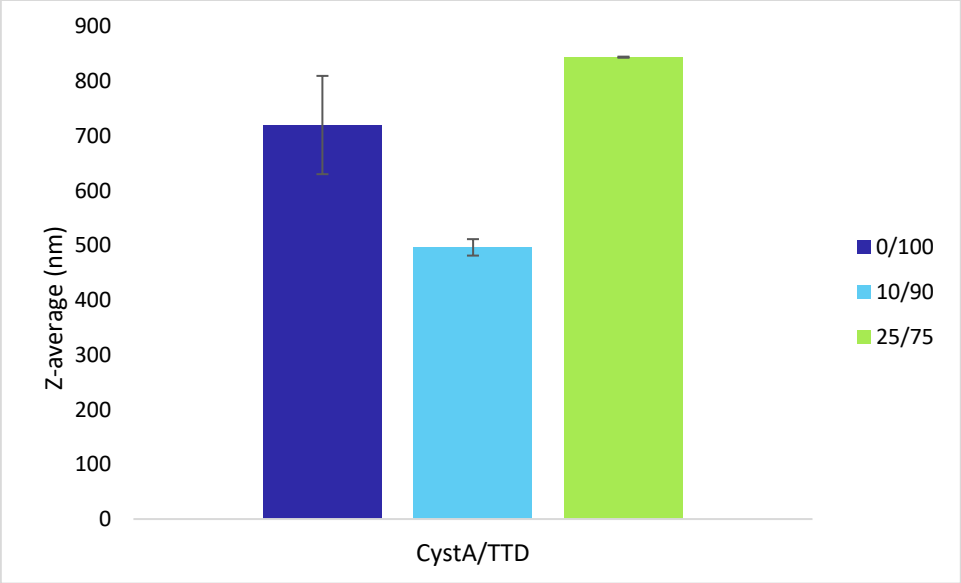

Figure 5.3 Z-average of CMA nanogels made with varied amounts of CystA/TTD. N=3, error bars: std. dev.

5.4.3 TMPTA/TTD gels with varied monomer wt%

Polymerized solutions of TMPTA/TTD with varied monomer feed wt%, 45, 30, 20, 10, 5 wt% were evaluated to investigate gelation. Samples with 10 or above wt% monomer were gelated, while the 5 wt% samples had a slightly opaque appearance (Figure 5.4).

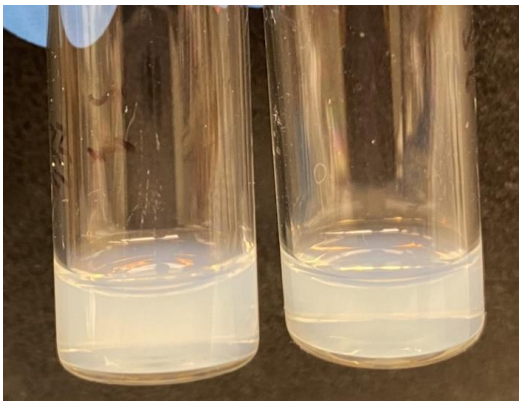
Figure 5.4 TMPTA/TTD 5 wt% samples.

5.4.4 TMPTA/PEG400DA nanogel synthesis

To determine an optimal monomer feed for nanogel formation, samples containing varied ratios of TMPTA/PEG were polymerized at varied concentrations, 10, 7, and 5 wt%. All 10wt% and 7 wt% 100/0 TMPTA/PEG400DA samples formed a bulk gel, while the remaining samples remained in solution form. Solutions were analyzed via DLS to investigate possible nanogel formation.

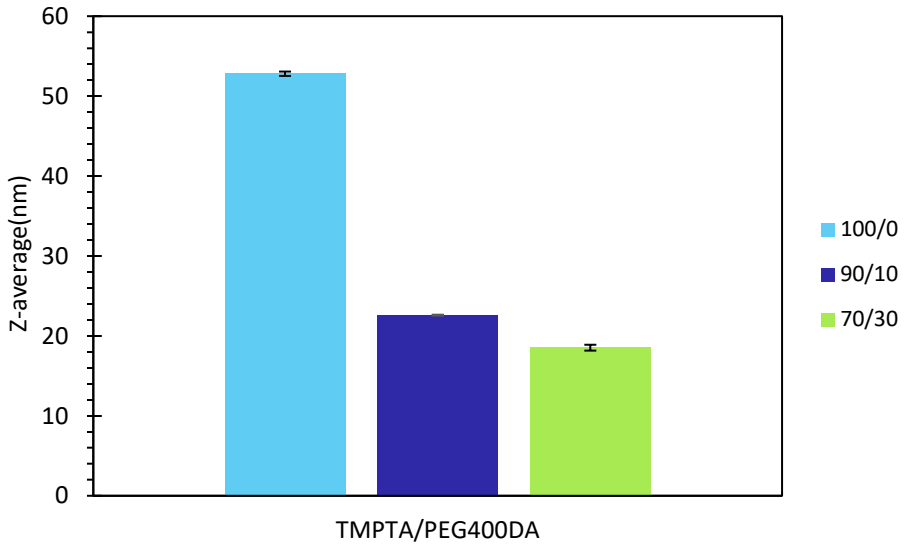

Figure 5.5 Z-average of nanogels made with a 5 wt% monomer feed and a varied TMPTA/PEG400DA ratio. N=3, error bars: std. dev.

Nanogels made with 100/0 TMPTA/PEG400DA were slightly larger than 90/10 and 70/30 TMPTA/PEG400DA, with a z-average of 53 nm compared to 22 nm and 18 nm respectively.

5.4.5 TMPTA/PEG400DA nanogels with varied CystA/TTD

To determine the disulfide bond's impact on the resulting networks' size, 90/10 TMPTA/TTD nanogels were synthesized from a 5wt% solution with 0/100 and 25/75 CystA/TTD (Figure 5.6). Nanogels without cystamine, 0/100 CystA/TTD, had a lower z-average of 22 nm compared to 25/75 CystA/TTD nanogels which had a z-average of 41 nm.

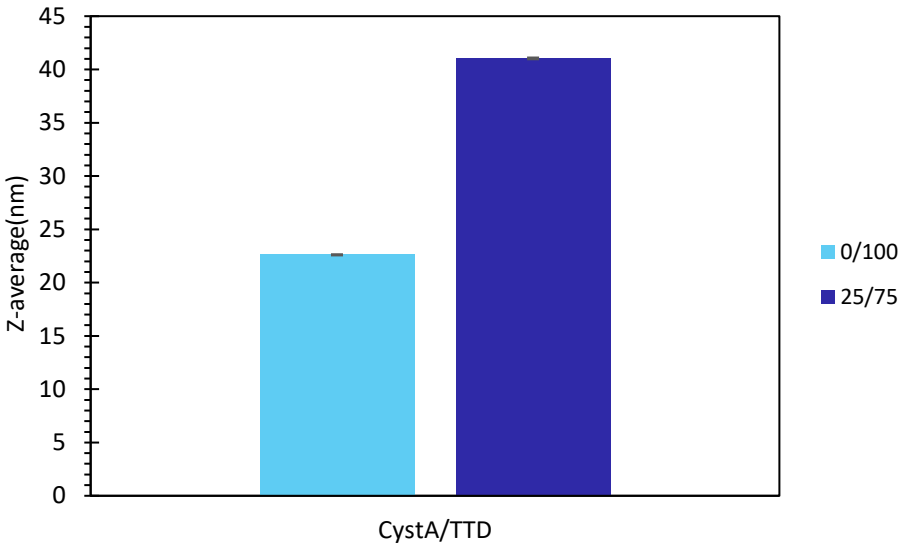

Figure 5.6 Z-average of nanogels made with a 5 wt% monomer feed, 90/10 TMPTA/PEG400DA and a varied TMPTA/PEG400DA ratio. N=3, error bars: std. dev.

5.5 Discussion

This study aimed to determine optimal parameters for PBAE nano gel formation. We started by looking at the DEGDA-containing PBAE systems; we had previously fabricated thin films made with 45wt % DEGDA and TTD monomer feed and hypothesized the analogous nano system formation in dilute conditions. The monomer feed was gradually lowered to determine the concentration beyond which no bulk gelation occurs. The solution

made with 5wt% did not gelate. However, no nanogel was detected by DLS. To better understand, the reaction kinetics of 5 wt% solutions were measured by monitoring DEGDA consumption, which indicated that over 98% of diacrylate had been consumed during 48 hrs of the reaction, which suggests the formation of oligomers rather than crosslinked polymers. These findings align with the literature, where Korshak et al. noted that diacrylate formed oligomers when polymerized in dilute conditions[64]. To aim to form crosslinked networks, we increased the functionality of an acrylate. Here, we successfully fabricated disulfide-containing PBAE systems using CMA with an acrylate functionality of 2.5, which supports the hypothesis that increased acrylate functionality enables the formation of nanogels. We further expanded on this concept with using blends of TMPTA and PEG400DA to form nanogels. We previously observed that highly crosslinked TMPTA networks were nondegradable as thin films. Thus, PEG400DA was introduced to increase degradability without significantly lowering average acrylate functionality. The data obtained by DLS suggests the formation of nanogels. However, further analysis is needed to characterize these networks.

5.6 Conclusion

Average acrylate functionality is an essential constraint in nano gel formation via Michael's addition in dilute conditions. Acrylate functionality can be increased by using solely branched monomers, such as triacrylate, TMPTA or a mixture or di/tri acrylate monomers. Here, we developed disulfide-containing PBAE nanogels by increasing the average acrylate functionality above 2.

Chapter 6. Conclusion and Future Directions

Tunable biomaterials are becoming increasingly advantageous due to their ability to be easily customized to meet specific needs. In this study, we expanded on the impact of acrylate properties, such as functional and hydrophilicity, on the formation and properties of the resulting PBAE networks. We demonstrated how the degradation can be increased from hours to days solely by changing the fraction of an acrylate. In addition, we designed GSH-responsive PBAE networks, which can be further used for various cellular delivery mechanisms. One of such mechanisms is nanogel, which we were able to synthesize by optimizing the monomer concentration and acrylate functionality and hydrophilicity. Future directions for this work can include cytotoxicity assessment of these nanogels and their degradation products, degradation studies, and their responsiveness to ROS in disulfide and free thiol forms.

References

1. Pepelanova, I., *Tunable Hydrogels: Introduction to the World of Smart Materials for Biomedical Applications.* Adv Biochem Eng Biotechnol, 2021. **178**: p. 1-35.
2. Goonoo, N., *Tunable biomaterials for myocardial tissue regeneration: promising new strategies for advanced biointerface control and improved therapeutic outcomes.* Biomater Sci, 2022. **10**(7): p. 1626-1646.
3. Ullah, A. and S.I. Lim, *Bioinspired tunable hydrogels: An update on methods of preparation, classification, and biomedical and therapeutic applications.* Int J Pharm, 2022. **612**: p. 121368.
4. Baawad, A., et al., *Rheological properties and decomposition rates of Gellan gum/hyaluronic acid/beta-tricalcium phosphate mixtures.* Int J Biol Macromol, 2022. **211**: p. 15-25.
5. Dhameri, S.A.A., *Rheological Properties and Decomposition Rates of Gellan Gum*. 2019, University of Toledo.
6. Forman, H.J., H. Zhang, and A. Rinna, *Glutathione: overview of its protective roles, measurement, and biosynthesis.* Mol Aspects Med, 2009. **30**(1-2): p. 1-12.
7. Meister, A., *Biosynthesis and functions of glutathione, an essential biofactor.* (0301-4800 (Print)).
8. Pizzorno, J., *Glutathione!* (1546-993X (Print)).
9. Sun, Y., et al., *Glutathione depletion induces ferroptosis, autophagy, and premature cell senescence in retinal pigment epithelial cells.* Cell Death & Disease, 2018. **9**(7): p. 753.
10. Franco, R. and J.A. Cidlowski, *Apoptosis and glutathione: beyond an antioxidant.* Cell Death & Differentiation, 2009. **16**(10): p. 1303-1314.
11. Sies, H., *Glutathione and its role in cellular functions.* Free Radical Biology and Medicine, 1999. **27**(9): p. 916-921.
12. Jones, D.P., *[11] Redox potential of GSH/GSSG couple: Assay and biological significance*, in *Methods in Enzymology*, H. Sies and L. Packer, Editors. 2002, Academic Press. p. 93-112.
13. Griffith, O.W., *Biologic and pharmacologic regulation of mammalian glutathione synthesis.* Free Radical Biology and Medicine, 1999. **27**(9): p. 922-935.
14. Wu, G., et al., *Glutathione metabolism and its implications for health.* J Nutr, 2004. **134**(3): p. 489-92.
15. Desideri, E., F. Ciccarone, and M.R. Ciriolo, *Targeting Glutathione Metabolism: Partner in Crime in Anticancer Therapy.* Nutrients, 2019. **11**(8).
16. Li, W., M. Li, and J. Qi, *Nano-Drug Design Based on the Physiological Properties of Glutathione.* Molecules, 2021. **26**(18).
17. Liu, Y., et al., *Poly(beta-Amino Esters): Synthesis, Formulations, and Their Biomedical Applications.* Adv Healthc Mater, 2019. **8**(2): p. e1801359.
18. Perni, S. and P. Prokopovich, *Poly-beta-amino-esters nano-vehicles based drug delivery system for cartilage.* Nanomedicine, 2017. **13**(2): p. 539-548.
19. Karlsson, J., et al., *Poly(beta-amino ester)s as gene delivery vehicles: challenges and opportunities.* Expert Opin Drug Deliv, 2020. **17**(10): p. 1395-1410.
20. Muralidharan, A., R.R. McLeod, and S.J. Bryant, *Hydrolytically degradable Poly (beta-amino ester) resins with tunable degradation for 3D printing by projection micro-stereolithography.* Adv Funct Mater, 2022. **32**(6).

21. Gupta, P., et al., *Quercetin conjugated poly(beta-amino esters) nanogels for the treatment of cellular oxidative stress.* Acta Biomater, 2015. **27**: p. 194-204.
22. Gupta, P., et al., *Controlled curcumin release via conjugation into PBAE nanogels enhances mitochondrial protection against oxidative stress.* Int J Pharm, 2016. **511**(2): p. 1012-21.
23. Biswal, D., et al., *A single-step polymerization method for poly(β-amino ester) biodegradable hydrogels.* Polymer, 2011. **52**(26): p. 5985-5992.
24. Lakes, A.L., et al., *Reducible disulfide poly(beta-amino ester) hydrogels for antioxidant delivery.* Acta Biomater, 2018. **68**: p. 178-189.
25. Scott, R.A. and N.A. Peppas, *Highly crosslinked, PEG-containing copolymers for sustained solute delivery.* Biomaterials, 1999. **20**(15): p. 1371-80.
26. Hawkins, A.M., N.S. Satarkar, and J.Z. Hilt, *Nanocomposite degradable hydrogels: demonstration of remote controlled degradation and drug release.* Pharm Res, 2009. **26**(3): p. 667-73.
27. Zitka, O., et al., *Redox status expressed as GSH:GSSG ratio as a marker for oxidative stress in paediatric tumour patients.* Oncol Lett, 2012. **4**(6): p. 1247-1253.
28. Sentellas, S., et al., *GSSG/GSH ratios in cryopreserved rat and human hepatocytes as a biomarker for drug induced oxidative stress.* Toxicology in Vitro, 2014. **28**(5): p. 1006-1015.
29. Kankaya, S., et al., *Glutathione-related antioxidant defence, DNA damage, and DNA repair in patients suffering from post-COVID conditions.* Mutagenesis, 2023. **38**(4): p. 216-226.
30. Chatterjee, A., *Reduced glutathione: a radioprotector or a modulator of DNA-repair activity?* Nutrients, 2013. **5**(2): p. 525-42.
31. Bej, R. and S. Ghosh, *Glutathione Triggered Cascade Degradation of an Amphiphilic Poly(disulfide)–Drug Conjugate and Targeted Release.* Bioconjugate Chemistry, 2019. **30**(1): p. 101-110.
32. Guo, X., et al., *Advances in redox-responsive drug delivery systems of tumor microenvironment.* J Nanobiotechnology, 2018. **16**(1): p. 74.
33. Yadav, S., et al. *Redox-Responsive Comparison of Diselenide and Disulfide Core-Cross-Linked Micelles for Drug Delivery Application*. Pharmaceutics, 2023. **15**, DOI: 10.3390/pharmaceutics15041159.
34. Troyano, A., et al., *Effect of glutathione depletion on antitumor drug toxicity (apoptosis and necrosis)in U-937 human promonocytic cells. The role of intracellular oxidation*. 2001, American Society for Biochemistry and Molecular Biology.
35. Smyth, J.F., et al., *Glutathione reduces the toxicity and improves quality of life of women diagnosed with ovarian cancer treated with cisplatin: results of a double-blind, randomised trial.* Ann Oncol, 1997. **8**(6): p. 569-73.
36. Xiong, Y., et al., *Engineering nanomedicine for glutathione depletion-augmented cancer therapy.* Chemical Society Reviews, 2021. **50**(10): p. 6013-6041.
37. Zhou, Z., et al., *GSH depletion liposome adjuvant for augmenting the photothermal immunotherapy of breast cancer.* Sci Adv, 2020. **6**(36).

38. Xu, Q., et al., *Injectable hyperbranched poly(β-amino ester) hydrogels with on-demand degradation profiles to match wound healing processes.* Chemical Science, 2018. **9**(8): p. 2179-2187.
39. Wiegman, K., et al., *Development of branched polyphenolic poly(beta amino esters) to facilitate post-synthesis processing.* Journal of Biomedical Materials Research Part B: Applied Biomaterials, 2022. **110**(12): p. 2714-2726.
40. Filipovic, V.V., et al., *Biodegradable Hydrogel Scaffolds Based on 2-Hydroxyethyl Methacrylate, Gelatin, Poly(beta-amino esters), and Hydroxyapatite.* Polymers (Basel), 2021. **14**(1).
41. Rekowska, N., et al. *Influence of PEGDA Molecular Weight and Concentration on the In Vitro Release of the Model Protein BSA–FITC from Photo Crosslinked Systems*. Pharmaceutics, 2023. **15**, DOI: 10.3390/pharmaceutics15041039.
42. Brey, D.M., I. Erickson, and J.A. Burdick, *Influence of macromer molecular weight and chemistry on poly(β-amino ester) network properties and initial cell interactions.* Journal of Biomedical Materials Research Part A, 2008. **85A**(3): p. 731-741.
43. Anderson, D.G., et al., *A Combinatorial Library of Photocrosslinkable and Degradable Materials.* Advanced Materials, 2006. **18**(19): p. 2614-2618.
44. Brey, D.M., et al., *Controlling poly(β-amino ester) network properties through macromer branching.* Acta Biomaterialia, 2008. **4**(2): p. 207-217.
45. Aguanell, A., et al., *Chitosan sulfate-lysozyme hybrid hydrogels as platforms with fine-tuned degradability and sustained inherent antibiotic and antioxidant activities.* Carbohydrate Polymers, 2022. **291**: p. 119611.
46. Tan, H., et al., *Controlled gelation and degradation rates of injectable hyaluronic acid-based hydrogels through a double crosslinking strategy.* J Tissue Eng Regen Med, 2011. **5**(10): p. 790-7.
47. Rich, M.H., et al., *Water–Hydrogel Binding Affinity Modulates Freeze-Drying-Induced Micropore Architecture and Skeletal Myotube Formation.* Biomacromolecules, 2015. **16**(8): p. 2255-2264.
48. Yang, X., et al., *Influence of crosslink on the formation of hydrophobic hydrogels.* Polymer Testing, 2023. **124**: p. 108103.
49. Navarro, R.S., et al., *Tuning Polymer Hydrophilicity to Regulate Gel Mechanics and Encapsulated Cell Morphology.* Adv Healthc Mater, 2022. **11**(13): p. e2200011.
50. Yeh, C.-C., A. Venault, and Y. Chang, *Structural effect of poly(ethylene glycol) segmental length on biofouling and hemocompatibility.* Polymer Journal, 2016. **48**(4): p. 551-558.
51. Krongauz, V.V., *Crosslink density dependence of polymer degradation kinetics: Photocrosslinked acrylates.* Thermochimica Acta, 2010. **503-504**: p. 70-84.
52. Holloway, J.L., et al., *Modulating hydrogel crosslink density and degradation to control bone morphogenetic protein delivery and in vivo bone formation.* J Control Release, 2014. **191**: p. 63-70.
53. Khakshoor, O. and J.S. Nowick, *Use of disulfide "staples" to stabilize beta-sheet quaternary structure.* Org Lett, 2009. **11**(14): p. 3000-3.

54. Niaz, S., B. Forbes, and B.T. Raimi-Abraham *Exploiting Endocytosis for Non-Spherical Nanoparticle Cellular Uptake*. Nanomanufacturing, 2022. **2**, 1-16 DOI: 10.3390/nanomanufacturing2010001.
55. Kou, L., et al., *The endocytosis and intracellular fate of nanomedicines: Implication for rational design.* Asian Journal of Pharmaceutical Sciences, 2013. **8**(1): p. 1-10.
56. Sousa de Almeida, M., et al., *Understanding nanoparticle endocytosis to improve targeting strategies in nanomedicine.* Chem Soc Rev, 2021. **50**(9): p. 5397-5434.
57. Aldayel, A.M., et al., *Effect of nanoparticle size on their distribution and retention in chronic inflammation sites.* Discover Nano, 2023. **18**(1): p. 105.
58. Hoshyar, N., et al., *The effect of nanoparticle size on in vivo pharmacokinetics and cellular interaction.* Nanomedicine (Lond), 2016. **11**(6): p. 673-92.
59. Gunasekaran, T., et al., *Nanotechnology: an effective tool for enhancing bioavailability and bioactivity of phytomedicine.* Asian Pac J Trop Biomed, 2014. **4**(Suppl 1): p. S1-7.
60. Kohane, D.S., *Microparticles and nanoparticles for drug delivery.* Biotechnol Bioeng, 2007. **96**(2): p. 203-9.
61. Rizvi, S.A.A. and A.M. Saleh, *Applications of nanoparticle systems in drug delivery technology.* Saudi Pharm J, 2018. **26**(1): p. 64-70.
62. Attama, A.A., et al., *Nanogels as target drug delivery systems in cancer therapy: A review of the last decade.* Front Pharmacol, 2022. **13**: p. 874510.
63. Namiot, E.D., et al., *Nanoparticles in Clinical Trials: Analysis of Clinical Trials, FDA Approvals and Use for COVID-19 Vaccines.* Int J Mol Sci, 2023. **24**(1).
64. Korshak, V.V., *Functionality of monomers and structure of polymers obtained by polycondensation. Review.* Polymer Science U.S.S.R., 1982. **24**(8): p. 1783-1797.

VITA

Education

University of Kentucky – Lexington, Kentucky.

M.S. Chemical Engineering (GPA: 3.73/4.0) expected

University of Toledo – Toledo, Ohio.

Bachelor of Arts (B.A.) Chemistry(GPA: 3.3/4.0)

Professional Experience

Research Assistant

January 2021– May 2024

Chemical and Materials Engineering Department, University of Kentucky, Lexington, Kentucky.

Chemistry Tutor

January 2018 – August 2018

University of Toledo, Toledo, Ohio.